Heat Transfer and Fluid Flow Characteristics Study for In-Line Tube Bank in Cross-Flow

Igbinosa Ikpotokin, Christian Okechukwu Osueke
Department of Mechanical Engineering, Landmark University, Omu-Aran, Kwara State Nigeria

***Abstract*-- This research investigates the heat transfer coefficient as a function of tube position and pressure drop, for in-line tube bank in cross-flow. Experimentation was essentially used to generate log-mean temperature curves and pressure heads upstream and down stream of the test section. The heat transfer and flow parameters such as Nusselt number, Reynolds number, and pressure drop across the bank were calculated. In addition, heat transfer correlations, Nusselt number (*Nu*) were obtained by power-law curve fitting for each position of the tube in the tube bank. FEMLAB 3.0 was use for numerical simulation and the results obtained compared favourably with that of the experimental results. Numerical results also reveal the important aspects of the local heat transfer and flow features within the tube bank. These characteristics include boundary layer developments between tubes, formation of vortices, local variations of the velocity and temperature distribution.**

***Index Term*-- In-line tube bank, cross-flow, flow characteristics.**

INTRODUCTION

Tube bank is a very important heat transfer surface used in many heat exchangers such as boilers for steam generation, radiators in automotive, fuel assemblies in nuclear power plants, cooling coils in air conditioning system. It consists of parallel cylindrical tubes that are heated by the fluid flow normal to it. Thereby, simulating a typical cross flow heat exchanger used in many engineering fields.

The tubes are usually arranged as in-line or staggered in the direction of fluid flow. In the former configuration, column of tubes is placed exactly behind the next adjacent column along the streamwise direction, without displacement in the cross-flow direction. For staggered tube configuration, every second column of tubes is displaced in the flow direction.

For this study, in-line tube bank is investigated. It is made up of four columns of five parallel cylinders. The configuration is characterized by the tube diameter and longitudinal and transverse pitches. The heat transfer characteristics associated with a tube is dependent on its position in the bank. This is as a result of the need to save space or energy in many engineering applications of energy conversion systems. Thus, prediction of heat transfer and flow characteristics at every tube position is required for determining the optimal design, efficient performance and operating parameters of compact heat exchangers. Since changes in properties associated with fluid flow over tube surfaces can result in losses and poor device performance (Yukio et al, 2010).

The fluid flow conditions within the bank are dominated by turbulence because of the high Reynolds numbers and induced vortex shedding which enhances the heat transfer process. The turbulence intensity and its generation are determined by the bank geometry and Reynolds number. It has been observed that with lower transverse pitches, the velocity fluctuations become more intensive (Yoo et al, 2007). Therefore, a tube bank acts as a turbulent grid and establishes a particular level of turbulence. The heat transfer condition stabilize, such that little change occurs in the convection coefficient for tube beyond the fifth row tube in staggered tube bank (Mehrabian, 2007).

Although reasonable number of researches have been conducted on experiments and numerical studies on fluid flow and heat transfer for tube bank, but different correlation equations have been proposed to predict the heat transfer or the Nusselt number. Majority of the correlations were based on overall heat transfer in the tube bank. Žukauskas obtained an overall heat transfer correlation given as

$$Nu = 0.52\,\mathrm{Re}^{0.5} \qquad 1$$

for in-line tube containing 16 number of tube rows (John et al, 2006).

From the numerous literatures, little or no work has been conducted to develop heat transfer correlation as a function of tube position for in-line tube bank.

Generally, a correction factor is always introduced in heat transfer coefficient correlation for number of tube rows because the shorter the bank, the lower the average heat transfer. The influence of the number of tube column becomes negligible only for N>16 (Incropera and Dewitt 2004).

The pressure drop in tube-type heat exchanger is related to the drag coefficient according to the following equation.

$$\Delta P = C_D N_{column} \frac{1}{2} \rho V^2 \qquad 2$$

Chunlei et al (2009) carried out a numerical study to determine the effect of tube spacing on flow characteristics for a six-row inline tube bank under laminar flow conditions (Re < 100). Their findings show that increasing tube space induces vortex shedding beginning from the last cylinder upstream.

The purpose of this study is to determine the pressure drop and average heat transfer characteristics at various tube positions and Reynolds number. Experiment was

conducted in cross-flow heat exchanger test apparatus. In addition, numerical simulation of two-dimensional fluid flow and heat transfer over the tube bank was performed and compared with the experimental data.

MATERIALS AND METHODS

Experimental procedure

The experimental procedure was used to generate cooling curves of the heated element for different flow conditions. The primary component of the test apparatus is valve controlled air flow duct with a perspex test section of 125mm x 125mm (Fig. 2) through which air is drawn by a centrifugal fan, and the heated element under investigation is inserted as shown in Fig 1.

Air temperature upstream of the test section and atmospheric pressure were measured by means of thermocouple and mercury barometer respectively. Air pressure differential across the test section were measured by inclined water manometer connected to the head tube located in the centre upstream position with the tube itself on the horizontal centerline of the test section as shown in Fig 1. The velocity upstream the test section was established from the pressure drop between atmosphere and upstream static pressure tapping (i.e depression of water column the manometer) and it was recorded as H_1 in meters. The sampled result is as shown in Table III.

Heat transfer measurements were obtained by replacing one of the Perspex rods with an externally identical heated copper rod. The copper rod outer and inner diameter is 12.45mm and 11.5mm respectively and its length is 95mm. It is carried between two extension rods of fabricated plastic compound. The element temperature is measured by K-type 0.2 mm diameter thermocouple probe inserted at its centre. The thermocouple output was connected to a digital multimeter (MAS-34X model) which also was connected to a Pentium 3 desktop computer as shown in Fig 1.

The test procedure involved heating the copper rod with electrical heater to 70^0C above air flow temperature outside the test section. Thereafter, it was inserted at different desired positions in the test sections (i.e centre of 1st, 2nd, 3rd and 4th columns) under different flow conditions such as 10, 20, 30, 40, 50, 60, 70, 80, 90 and 100% throttle openings. Then its temperature and time of cooling were recorded with the thermocouple embedded at its centre. The heat transfer coefficient is then deduced from logarithm plot (Fig 3.0).

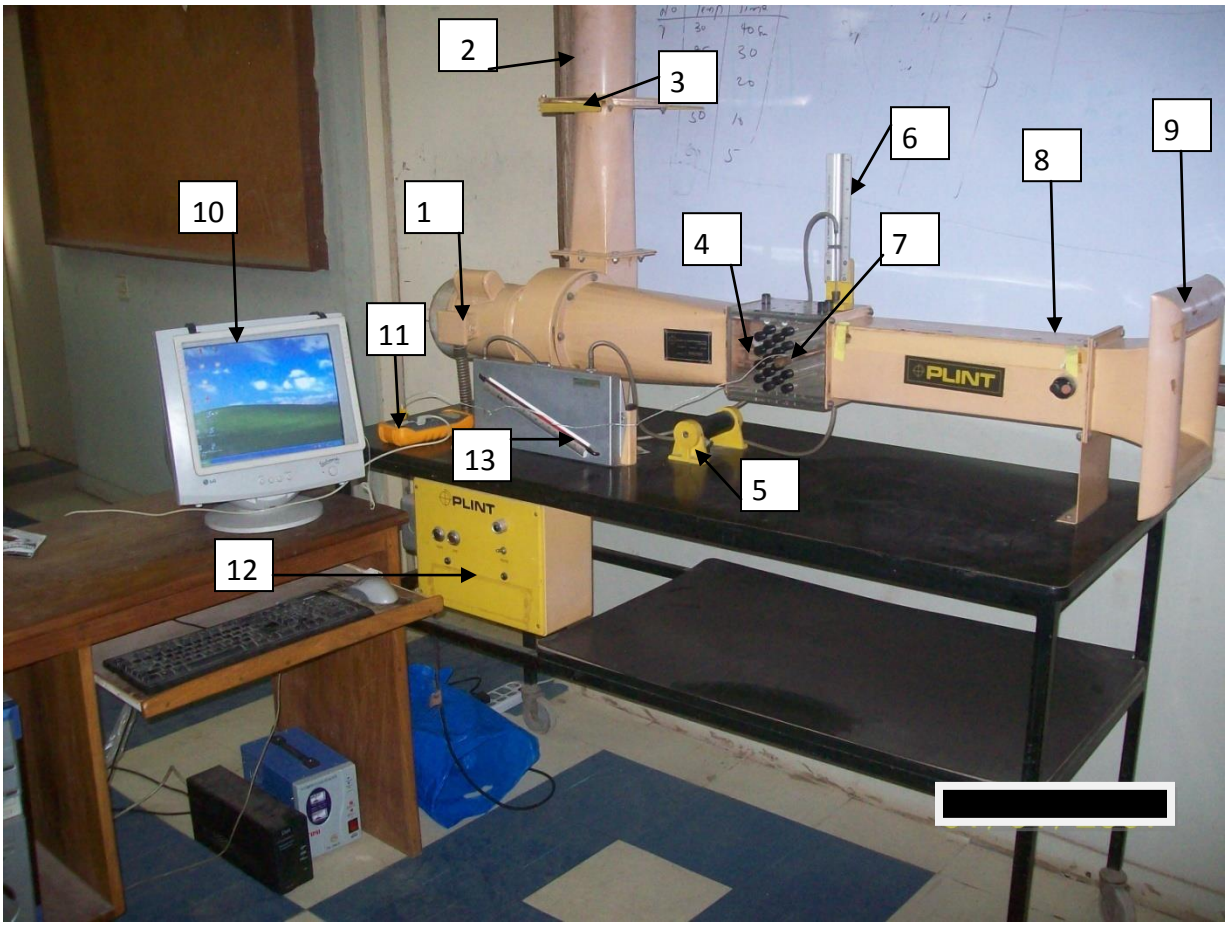

Fig.1. Cross flow experimental test apparatus.

The apparatus in Fig.1 are as identified by the numerals

1. Fan, 2. Air discharge tube, 3. Throttle valve, 4. Test section, 5. Electric heater, 6. Total head tube, 7. Test element, 8. Thermometer, 9. Bellmouth, 10. Computer, 11. Digital multimeter, 12. Control panel and 13. Inclined manometer.

Basic assumptions and problem formulation

It was assumed that the heat generated in the cylindrical copper element was transferred to the air flowing through it. However, a certain amount of heat was conducted from the element into the plastic extension pieces. A correction factor of 8.4mm was used to compensate for plastic extension. Therefore:

$L_1 = L + 0.0084$ 3

It was further assumed that temperature gradients within the element are negligible, so the thermocouple embedded at the centre gives a true reading of the effective surface temperature. The justification for this assumption is that the Biot number is very small ($Bi < 0.1$).

The rate of heat transfer from the element to the air stream is given by:

$q = hA(T - T_a)$ 4

The temperature drop dT in a period of time dt is given by:

$-qdt = mcdT$ 5

Combining Equations (4) and (5) gives:

$$\frac{-dT}{(T-T_a)} = \frac{hA_1}{mc}dt \qquad 6$$

where A is replaced by A_1 to allow for the tube plastic extensions. Integrating equation (6), we obtain:

$$\log_e(T-T_a) - \log_e(T_o - T_a) = \frac{-hA_1 t}{mc} \qquad 7$$

Equation (7) suggests that a plot of $\log_e(T-T_a)$ against t yield a straight line slope

$$M = \frac{-hA_1}{mc} \qquad 8$$

and since we can obtained the other factors in this expression from the geometrical properties of copper in Table I, the heat transfer coefficient relates to the slope M of the line by the following expression:

$$h = \frac{-mc}{A_1}M \qquad 9$$

A plot of $log_{10}(T - T_a)$ against time (t) was used, since $log_e N = 2.3026\ log_{10} N$.

The effective velocity of the air across the element was determined by calculating the velocity V_1 upstream. The velocity V_1 developed by gas of density ρ expanding freely from rest under the influence of pressure difference P. When P was sufficiently small for compressibility to be neglected, then, applying Bernoulli's equation gives:

$$\frac{\rho V_1^2}{2} = P \qquad 10a$$

the pressure head H_1 was measured in centimeters of water. Since

$1cm\ H_2O = 98.1\ N/m^2$ equation (10a) becomes

$$\frac{\ell V_1^2}{2} = 98.1H_1 \qquad 10b$$

The density of air under pressure P_a and at temperature T_a is given by ideal gas equation.

$P_a = RT_a$ 11

where the gas constant $R = 2875J/kmol.K$

substituting equation (10) in (11) yields:

$$V_1 = 237.3\sqrt{\frac{H_1 T_A}{P_A}} \qquad 12$$

Equation (12) is used for calculating local velocities upstream of the test section.

The calculation of the effective velocity through bank of tubes was based on the minimum flow area. When all the tubes are in position, the minimum area occurs in a transverse plane. Therefore,

$$V = 2V_1 \qquad 13$$

Dimensional analysis shows that the relationship between h and the independent variables is expressed as:

$$\frac{hD}{K} = Nu \qquad 14$$

$$\mathrm{Re} = \frac{\ell VD}{\mu} \qquad 15$$

The pressure differential was express as a proportion to the velocity head. It represents the pressure drop imposed on the flow by each successive rank of tubes which is represented as:

$$H_3 = H_1 - H_2 \qquad 16$$

and the drag coefficient is calculated as:

$$C_D = \frac{H_3}{4}/4H_1 \qquad 17$$

Thus, pressure drop across the tube bank is

$$\Delta P = C_D \frac{\rho V^2}{2} \qquad 18$$

NUMERICAL MODELLING

Numerical simulation was essential for flow visualization and temperature distribution in the tube bank. The simulation modeling was performed in a two-dimensional domain, which represents the test section as shown in Fig. 2. FEMLAB 3.0 software was used to draw all parts in computational domain and to generate grids. The dimensions

of computational domain were idealized to reveal the fundamental issues and enable validation with the experimental data that was the reason why this computational domain only cover the test working section. This computational domain has a length and width as same size with the experimental test section.

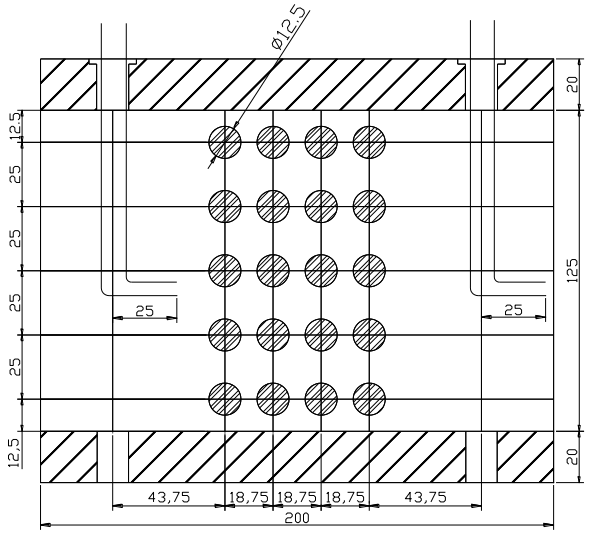

Fig. 2. Schematic diagram of the in-line tube bank test section.

Since the governing equations are in spatial coordinates, the boundary conditions were provided for all boundaries of the computation domain. At the up-stream boundary, uniform flow velocity U_{in} and temperature T_{in} were assumed. At the down-stream end of the computational domain, the Neumann boundary condition was applied. At the solid cylinder surfaces represented by circles, no-slip conditions and thermal insulation were applied, while constant temperature T_{tube} was specified for the heated element. At the symmetry plane, normal velocity and the temperature variation along the normal direction were set to zero.

RESULTS AND DISCUSSION

Experimental and numerical simulations of heat transfer and fluid flow characteristics of in-line tube bank are presented.

For these studies, the following dimensions and fluid properties used are presented in tables I and II respectively.

Table I
Geometrical properties of the copper rod.

Description	Quantity	Unit
External diameter (d)	12.45	mm
Internal diameter (d_i)	11.5	mm
Thickness of tube (t)	0.5	mm
Length of tube (l)	95	mm
Effective length (l_1)	0.1304	m
Surface area (A)	0.00371	m^2
Effective surface area (A_1)	0.00404	m^2
Specific heat (C)	380	J/kg.K
Mass (m)	0.0274	Kg

Table II
Properties of the fluid (air).

Description	Quantity	Unit
Ambient temperature (T_a)	300	^oK
Barometric pressure (P_a)	99,042	N/m^2
Density of air at T_a (ρ)	1.1614	kg/m^3
Dynamic viscosity (μ)	$1.846X10^{-5}$	kg/ms

Thermal conductivity (*K*) 0.0263 J/ms^{o}C

Experimental test was used to generate cooling curves. For example, the rate of cooling resulting from minimum flow rate set at 100% when the heated element was positioned in the center of the second column is shown in Fig 3. The slope obtained from the rate of cooling curve with the knowledge of element properties in Table I were used in equation 9 to calculate the convective heat transfer coefficient.

The above procedure was used to calculate the heat transfer characteristics from the heated element at 1st, 2nd, 3rd and 4th positions of the tube columns. The results obtained for different set flow rate in the ranges of 10 – 100% are presented in tables III, IV, V and VI. The effective velocity, V across the bank tube based on the minimum flow area was obtained from equation 13 and thee result is shown in table III. The pressure head differential, H_3 in cmH_2O imposed on the flow by each successive column of tube across the exchanger was obtained with all the tubes in position. The drag coefficient which is represented by the slope of the plot of H_1 against H_3 shown in Fig 4 was used in equation 17 to calculate the pressure drop across the tube bank and the result is presented in table VII. Fig.5 depicts a parabolic increase of pressure drop with increasing Reynolds number.

Table III
Data Corresponding to Ten Different Throttle Openings when the Heated Element is positioned at the Center of 1st column

Throttle opening (%)	H1 (cmH_20)	V_1 (m/s)	V (m/s)	Re	M (s^{-1})	h (J/ms^{2o}C)	Nu
10	0.03	2.263	4.524	3543	-0.008	47.48284	22.47762
20	0.18	5.541	11.082	8680	-0.0094	55.79234	26.4112
30	0.33	7.502	15.005	11753	-0.0106	62.91477	29.78285
40	0.48	9.048	18.097	14175	-0.0115	68.25659	32.31158
50	0.64	10.448	20.896	16367	-0.0119	70.63073	33.43546
60	0.79	11.608	23.216	18187	-0.0124	73.59841	34.84031
70	0.94	12.662	25.325	19836	-0.0126	74.78548	35.40225
80	1.096	13.673	27.345	21418	-0.0129	76.56609	36.24516
90	1.248	14.59	29.18	22856	-0.0132	78.34669	37.08807
100	1.42	15.563	31.126	24380	-0.0134	79.53376	37.65001

Table IV
Data Corresponding to Ten Different Throttle Openings when the Heated Element is positioned at the centre of 2nd column

Throttle opening (%)	H_1 (cmH_20)	V_1 (m/s)	V (m/s)	Re	M (s^{-1})	h (J/ms^oC)	Nu
10	0.03	2.263	4.524	3543	-0.0088	52.23113	24.72538
20	0.18	5.541	11.082	8680	-0.011	65.28891	30.90673
30	0.33	7.502	15.005	11753	-0.0123	73.00487	34.55934
40	0.48	9.048	18.097	14175	-0.013	77.15962	36.52613
50	0.64	10.448	20.896	16367	-0.0136	80.72083	38.21195
60	0.79	11.608	23.216	18187	-0.014	83.09498	39.33583
70	0.94	12.662	25.325	19836	-0.0142	84.28205	39.89778
80	1.096	13.673	27.345	21418	-0.0143	84.87558	40.17875
90	1.248	14.59	29.18	22856	-0.0144	85.46912	40.45972
100	1.42	15.563	31.126	24380	-0.0146	86.65619	41.02166

Table V
Data Corresponding to Ten Different Throttle Openings when the Heated Element is positioned at the Center of 3rd column

Throttle opening (%)	H_1 (cmH_20)	V_1 (m/s)	V (m/s)	Re	M (s^{-1})	h (J/ms^oC)	Nu
10	0.03	2.263	4.524	3543	-0.01	59.35355	28.09702
20	0.18	5.541	11.082	8680	-0.0127	75.37901	35.68322
30	0.33	7.502	15.005	11753	-0.0138	81.90791	38.77389
40	0.48	9.048	18.097	14175	-0.0141	83.68851	39.61681
50	0.64	10.448	20.896	16367	-0.0146	86.65619	41.02166
60	0.79	11.608	23.216	18187	-0.0153	90.81094	42.98845
70	0.94	12.662	25.325	19836	-0.0158	93.77862	44.3933
80	1.096	13.673	27.345	21418	-0.0162	96.15276	45.51718
90	1.248	14.59	29.18	22856	-0.0164	97.33983	46.07912
100	1.42	15.563	31.126	24380	-0.0166	98.5269	46.64106

Table VI

Data Corresponding to Ten Different Throttle Openings when the Heated Element is positioned at the Center of 4th column

Throttle opening (%)	H_1 (cmH_20)	V_1 (m/s)	V (m/s)	Re	M (s^{-1})	h (J/ms^oC)	Nu
10	0.03	2.263	4.524	3543	-0.011	65.28891	30.90673
20	0.18	5.541	11.082	8680	-0.0132	78.34669	37.08807
30	0.33	7.502	15.005	11753	-0.0144	85.46912	40.45972
40	0.48	9.048	18.097	14175	-0.0149	88.4368	41.86457
50	0.64	10.448	20.896	16367	-0.0157	93.18508	44.11233
60	0.79	11.608	23.216	18187	-0.016	94.96569	44.95524
70	0.94	12.662	25.325	19836	-0.0166	98.5269	46.64106
80	1.096	13.673	27.345	21418	-0.0169	100.3075	47.48397
90	1.248	14.59	29.18	22856	-0.017	100.901	47.76494
100	1.42	15.563	31.126	24380	-0.0172	102.0881	48.32688

Table VII

Pressure drop across the tube banks.

% throttle openings	Reynolds number (Re)	Pressure drop (ΔP) (N/m^2)
10	3543	13.734
20	8680	35.316
30	11753	100.062
40	14175	122.625
50	16367	145.188
60	18184	216.801
70	19836	247.212
80	21418	296.262
90	22856	327.654
100	24380	361.989

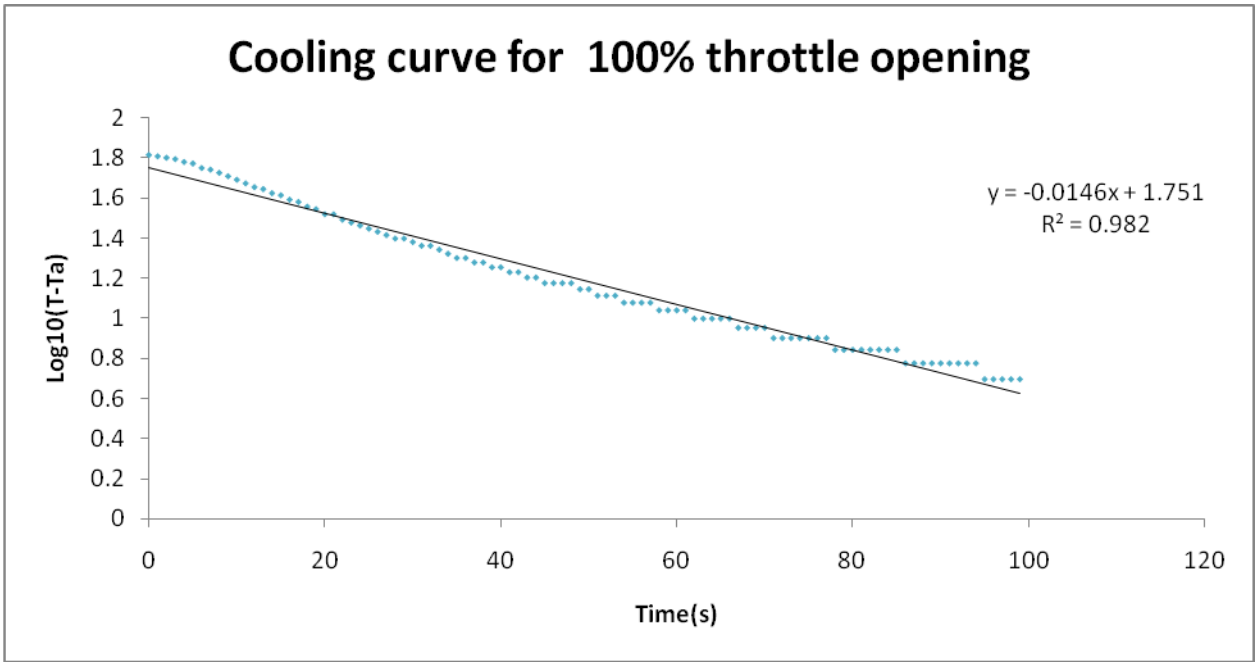

Fig. 3. A plot of $\log_{10}$(T-Ta) against t for 100% throttle opening.

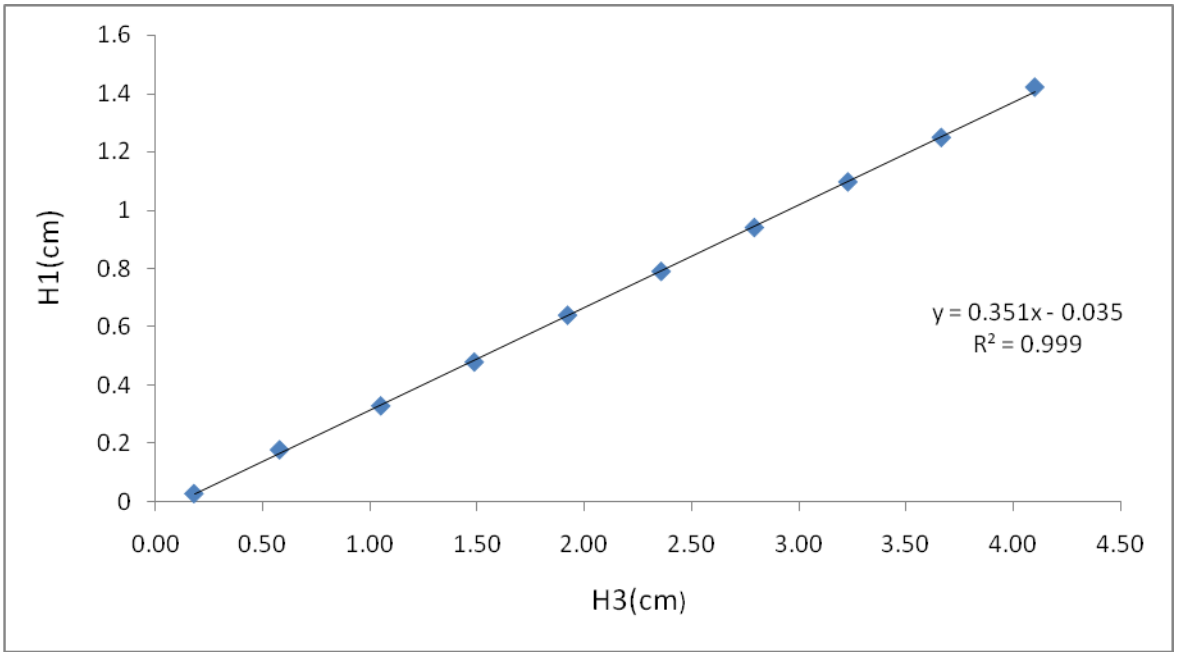

Fig. 4. Pressure head differential across the tube bank.

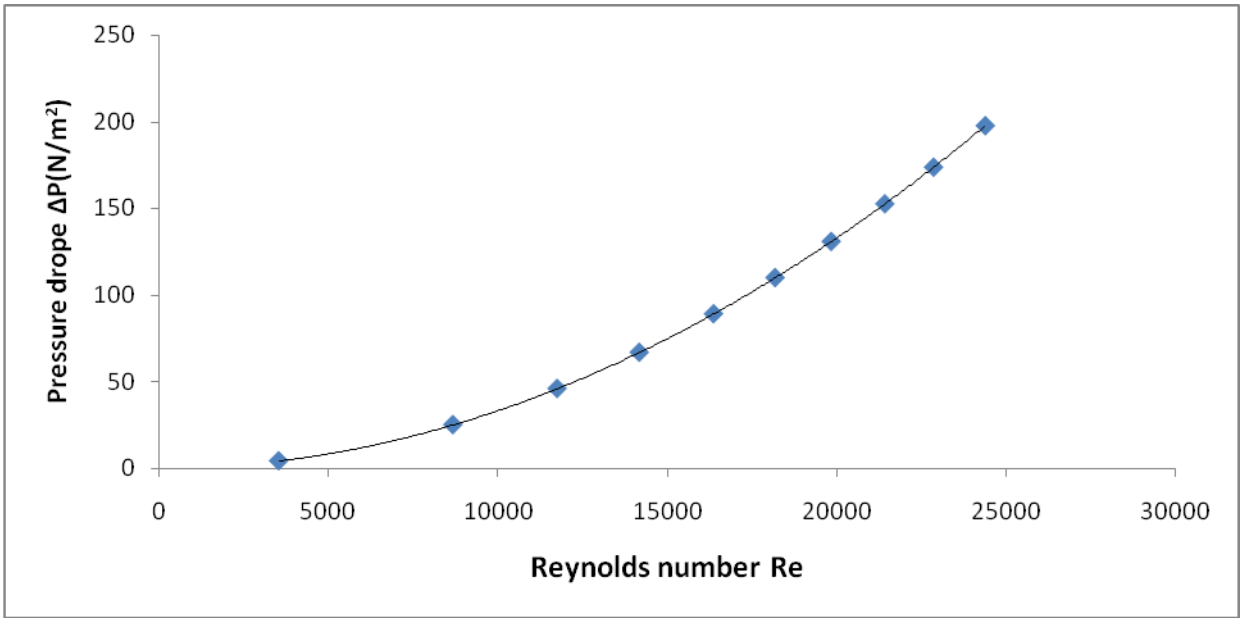

Fig. 5. Pressure drop across the tube bank

Dimensionless quantities such as Reynolds number and Nusselt number were calculated using equations 15 and 14 respectively and the results are shown in table III, IV, V and VI. Furthermore, empirical correlation for heat transfer coefficient was obtained with power-law curve fitting. The curves are shown in Fig. 6 and the resulting correlations are shown in table VIII.

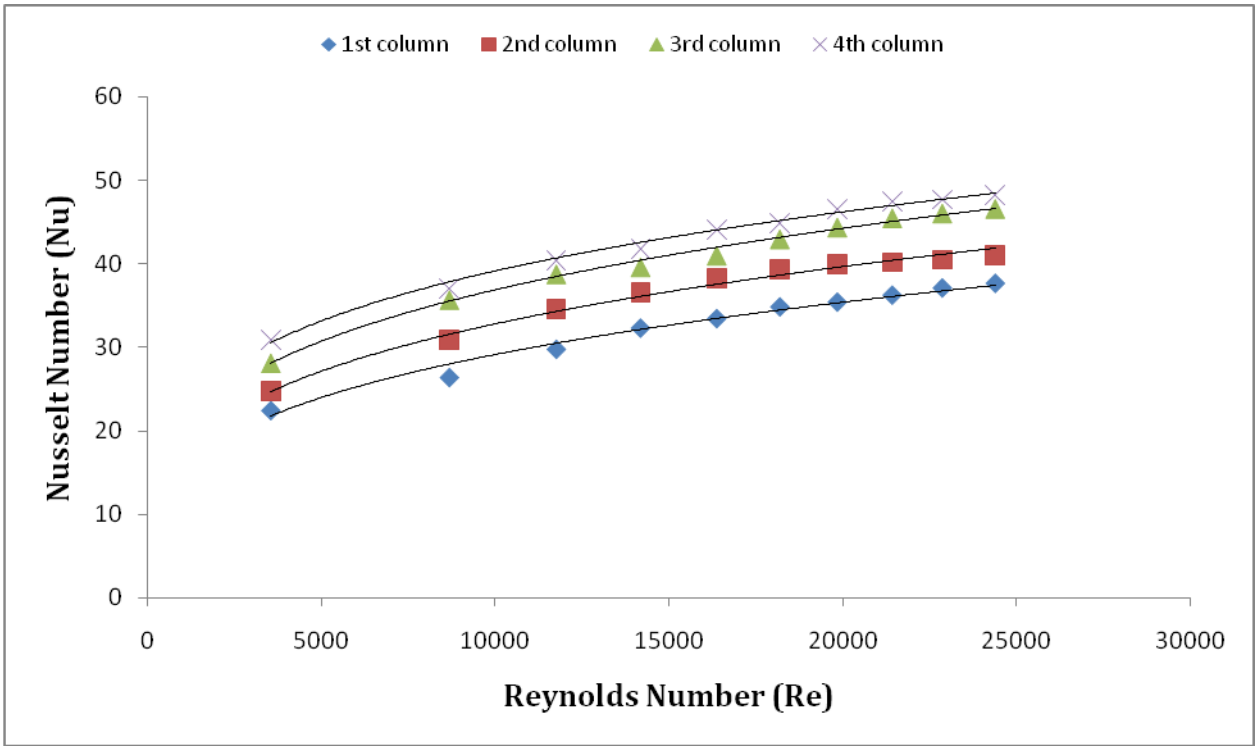

Fig. 6. Relationship between experimental *Nu* and *Re* for tube positions in the tube bank.

Table VIII
Experimental results showing Nu and Re relationship

Rows	Experimental Correlations
1st	$Nu = 4.302Re^{0.239}$, $R^2 = 0.978$
2nd	$Nu = 3.269Re^{0.262}$, $R^2 = 0.991$
3rd	$Nu = 2.672Re^{0.272}$, $R^2 = 0.994$
4th	$Nu = 2.178Re^{0.281}$, $R^2 = 0.993$

Numerical results Velocity Distribution

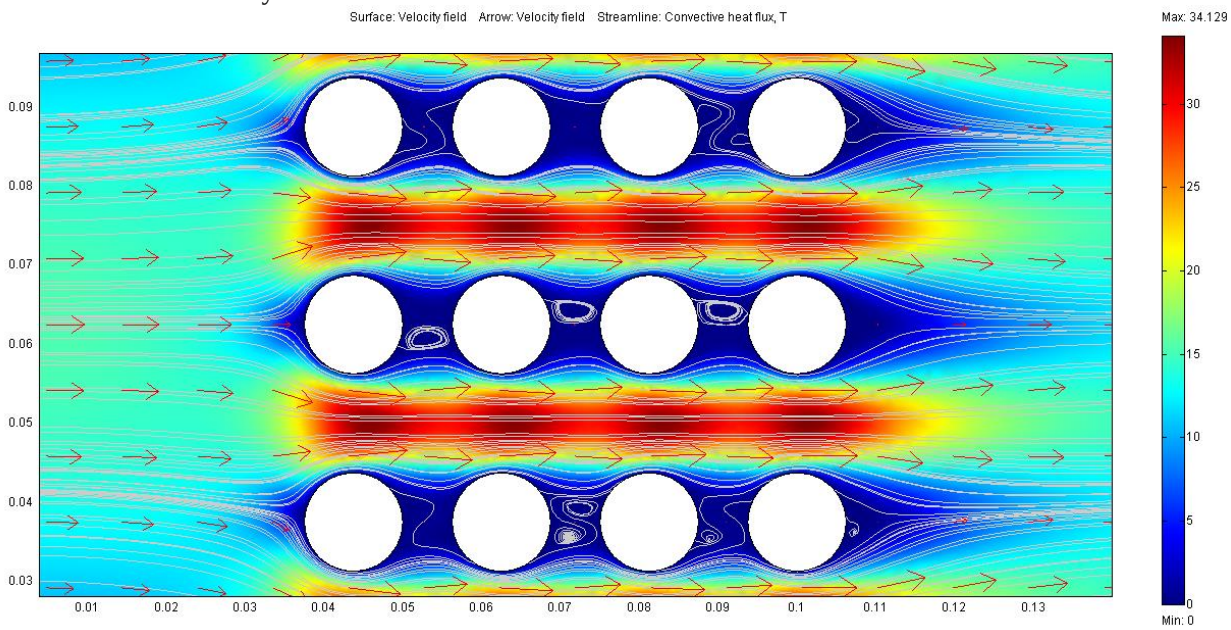

Fig. 7. Velocity distribution in the tube bank at Re = 24380

Velocity pattern in the bank is illustrated in Fig. 7. Fluid velocity in the mid-plane of the tubes was observed to be higher and weak near tube surface plane because of the boundary layer development on the surface.

As shown in Fig.7, a large portion of the tube surface area of only the first rank is exposed to the main flow. A larger flow recirculation region or dead zone is formed between the two adjacent tubes. It also proves clearly the existence of reverse flow patterns upstream of deeper rows. Furthermore, these velocity data confirm that a bypass stream exists between the tubes. Moreover, the active heat transfer surface area is small since the up and down stream parts of a tube surface are in the low velocity region. The streamline plot revealed that vortex formation occurs in the zones of recirculation. Maximum velocity was seen to occur at the minimum cross section.

Boundary Layer Separation

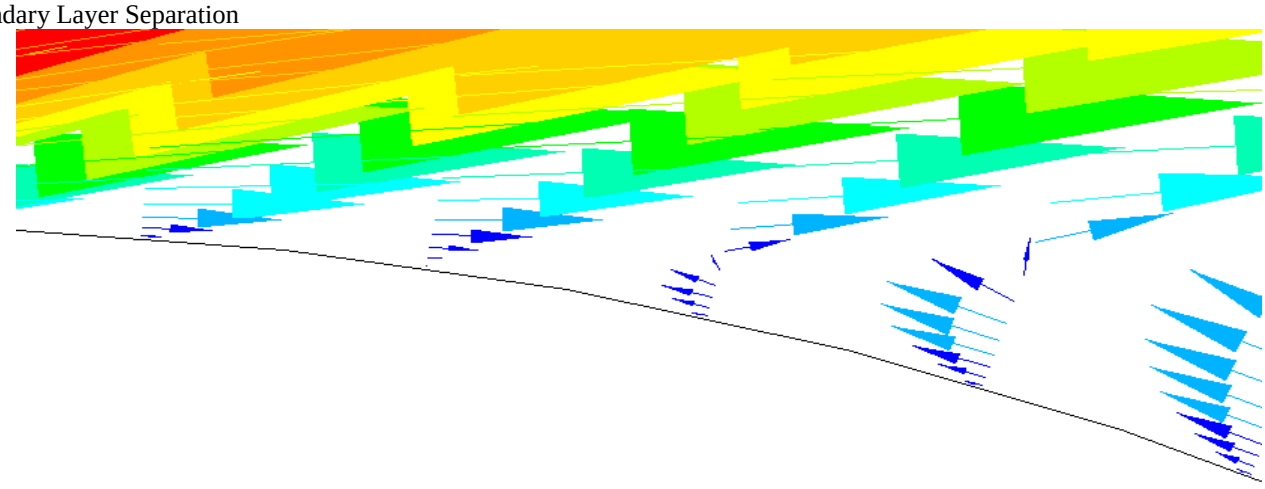

Fig. 8. The boundary layer separation point of first rank in tube bank at Re = 24380

Boundary layer separation occur at a point on the tubes where the fluid momentum is too weak to overcome the adverse pressure gradient and then detached from the tubes surface as shown in figure 8. This separation was observed shortly after ($\theta = 90°$). By the nature of these flow separations, local heat transfer and fluid mixing increase especially upstream of the tubes and cause low performance at the wake region located downstream of the tubes.

Temperature Distribution

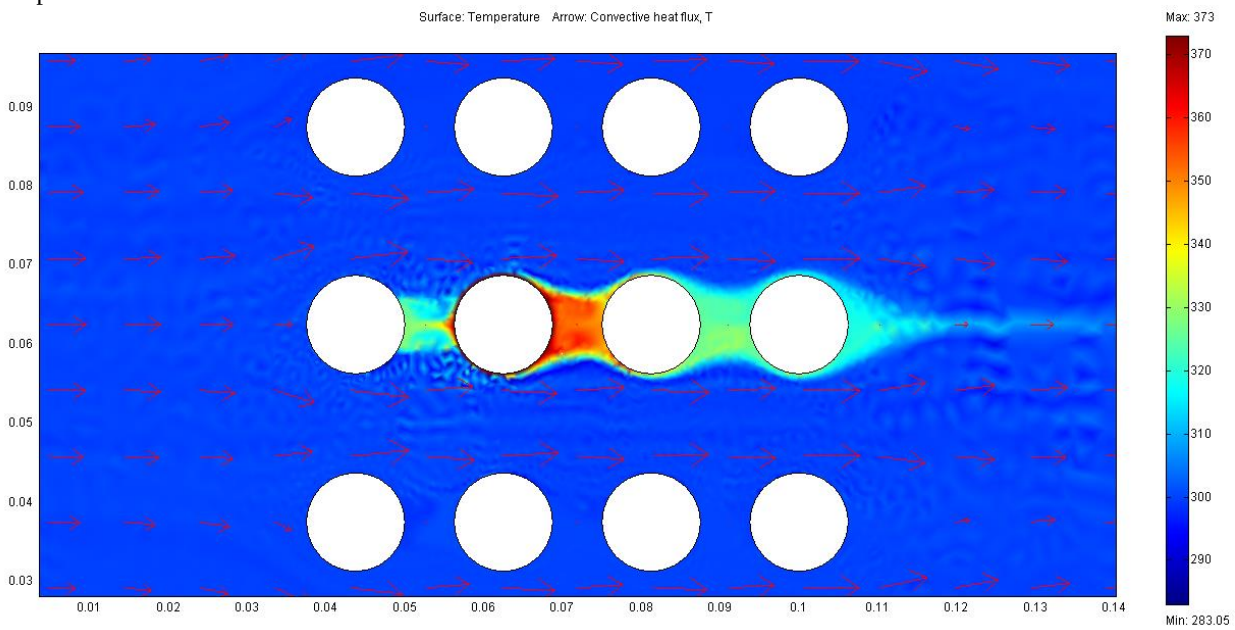

Fig. 9. Temperature distributions in the tube bank at Re = 24380.

Fig.9 shows the temperature distributions within the bank. The cooling rate of the heated element is grater within the tube-mid planes where maximum local velocity occurs. This was evident by the low temperature close to that of the free stream recorded. The temperature gradient near the upstream tube was higher due to the thin boundary layer thicken, while the temperature gradient down stream along the tube is lower than the upstream due to the wake flow.

The numerical data were essentially used to reveal temperature distribution and flow visualization such as velocity distribution, boundary layer separation occurring within the tube bank. The experimental test was used to generate cooling curves. A logarithm plot for the rate of cooling was produced as shown in Fig. 3. The slope obtained from Fig. 3.0, together with the knowledge of the copper thermal capacity, mass, and surface area were used to calculate heat transfer coefficient between the heated copper element, and the air flow normal to it.

Pressure drop across the tube-type heat exchanger increase with increasing Reynolds. Numerical results were 10% higher than the experimental.

It is observed that the heat transfer coefficient increases, though at a diminishing rate, in successive columns of tubes. This is caused by the increasing level of turbulence and stability as the air passes through the tube bank.

Numerical Nusselt number was 12% higher than that of the experimental results. The discrepancy in result could be due to poor convergence resulting from inability of the software to handle high turbulent flow that was obtained in the experimental work. Both the experimental and numerical predictions indicate that the Nusselt number and pressure drop increase with the increasing Reynolds number and also with the tube location in the bank.

CONCLUSION

The heat transfer coefficient from the heated element was found to be a function of its position and Reynolds number in the tube bank. Nusselt number increase by 12.49% from first to second column, 11.85% from second to third column and 5.27% from third to fourth column. This was due to increasing level of turbulence created by successive column of tubes as the air passes through the bank. However, the increments were at diminishing rate in successive column of tubes. Downstream from the third column, the heat transfer stabilizes, such that little change occurs in the convection coefficient from tube beyond the fourth. This will thus facilitate compact heat exchanger design and discourage the use of large number of tubes that to save space and energy.

Numerical and experimental results compared favourably. Flow visualization results for boundary layer developments and vortex formation between the tubes, and local velocity and temperature distributions in the tube bank were obtained by the present numerical simulation. The boundary layer developments and vortices between the adjacent tube surfaces were found to be strongly dependent on Reynolds number. Vortex formation occurs between column of tubes and downstream of the fourth column of tubes. This justifies increased resistance to heat transfer. The velocity distribution results indicate a strong bypass stream of fluid between the tubes occurs.

The present numerical and experimental investigations suggest that changes in heat transfer from copper tube was dependent on the position and flow pattern (Reynolds number) in the heat exchanger while the pressure drop was a function of the Reynolds numbers.

REFERENCES

[1] M. A. Mehrabian, 2007, Heat Transfer and Pressure Drop Characteristics Of Cross Flow Of Air Over An Circular Tube in Isolation And/Or in a Tube Bank, The Arabian Journal for Science and Engineering, Volume 32.

[2] S.Y. Yoo, H.K. Kwon, J.H. Kim, 2007, A study on heat transfer characteristics for staggered tube banks in cross-flow, J. Mech. Sci. Technol. Vol. 21 pp 505–512.

[3] Yukio Takemoto, Keiji Kawanishi, Jiro Mizushima, 2010, Heat transfer in the flow through a bundle of tubes and transitions of the flow, International Journal of Heat and Mass Transfer, Vol. 53 pp 5411–5419.

[4] Incropera, F.P. and Dewitt, D.P.(2004), Fundamental of Heat and Mass Transfer, 5th ed., John Wiley & Sons, Inc.

[5] John, H. Lienhard IV and John, H. Lienhard V (2006), A Heat Transfer Textbook, 3rd ed., Phlogiston Press, Cambridge, Massachusetts, USA

[6] Chunlei Liang , George Papadakis, Xiaoyu Luo (2009), Effect of tube spacing on the vortex shedding characteristics of laminar flow past an inline tube array: A numerical study, International Journal of Computers & Fluids, 38, 950–964